CHINESE OPTICS LETTERS

Vol. 21, No. 3 | March 2023

High color saturation and angle-insensitive ultrathin color filter based on effective medium theory

Xinting Li (李欣婷)[1], Yang Li (李 阳)[1,2], Chao Li (李 超)[1], Song Gao (高 嵩)[1,2*], and Wenjing Yue (岳文静)[1,2**]

[1] School of Information Science and Engineering, University of Jinan, Jinan 250022, China

[2] Shandong Provincial Key Laboratory of Network Based Intelligent Computing, University of Jinan, Jinan 250022, China

*Corresponding author: ise_gaos@ujn.edu.cn

**Corresponding author: ise_yuewj@ujn.edu.cn

Received June 28, 2022 | Accepted November 7, 2022 | Posted Online December 1, 2022

An ultrathin angle-insensitive color filter enabling high color saturation and a wide color gamut is proposed by relying on a magnesium hydride-hydrogenated amorphous silicon (MgH_2-a-Si:H) lossy dielectric layer. Based on effective medium theory, the MgH_2-a-Si:H layer with an ultrathin thickness can be equivalent to a quasi-homogeneous dielectric layer with an effective complex refractive index, which can be tuned by altering the thickness of MgH_2 to obtain the targeted value of the imaginary part, corresponding to the realization of high color saturation. It is verified that the proposed color filter offers highly enhanced color saturation in conjunction with a wide color gamut by introducing a few-nanometer thick MgH_2 layer. As the MgH_2-a-Si:H layer retains the advantages of high refractive index and tiny thickness, the proposed color filter exhibits large angular tolerance up to ±60°. In addition, MgH_2 with an unstable property can interconvert with Mg under a dehydrogenation/hydrogenation reaction, which empowers the proposed color filter with dynamically tunable output color. The proposed scheme shows great promise in color printing and ultracompact display devices with high color saturation, wide gamut, large angular tolerance, and dynamic tunability.

Keywords: color filter; effective medium theory; lossy dielectric layer; color saturation; angle insensitivity.

DOI: 10.3788/COL202321.033602

1. Introduction

Color filter is a crucial component of display/imaging devices, color printing, decoration, consumer products, etc., which dominantly determines the color quality, embracing color vibrancy, saturation, gamut, brightness, and resolution[1,2]. The conventional commercial color filter relies on the absorption characteristic of pigment/dye for a specific wavelength to generate a certain chemical color. The essence of chemical color totally depends on the intrinsic property of pigment/dye, so it is required to use different kinds of pigments/dyes to generate different colors. Additionally, the chemical color holds the disadvantages of being environmentally unfriendly and prone to fading, owing to the fact that the pigments/dyes are toxic and are quite sensitive to UV light and high temperatures. Given this, a nature-inspired method of physical color generation, namely, structural color that originates from physical phenomena such as scattering, interference, or diffraction excited by the interaction between light and nanostructures, has gained abundant attention[3,4]. This new color generation concept enables the generation of vivid colors by simply tuning the geometric parameters or arrangement of nanostructures, leading to a more flexible color toning method.

Until now, various configurations have been extensively researched to construct the color filters, such as nanoholes, nanodisks, nanopillars, and nanogratings[5–8]. However, the fabrication of these patterned nanostructures relies on a complicated and expensive lithography process, which prevents mass production and practical application. Moreover, the colors originating from the patterned nanostructure are greatly affected by the change in incident angle, which is not adequate for those devices requiring a wide field of view. To conquer the above-mentioned issues faced by the patterned nanostructures, a planar thin-film structure is preferred, as it can be easily manufactured via simple processes and industrially achieved on a large scale. Meanwhile, the planar thin-film structures can afford more relaxed angle tolerance[9,10]. A typical thin-film configuration to realize large-scale and angle-insensitive color filters is the metal-dielectric-metal (MDM) Fabry-Perot (FP) resonator that consists of a dielectric layer sandwiched between two metallic layers[11–13]. To further realize ultrathin devices, a simple thin-film structure composed of a dielectric layer made of

high-refractive-index lossy materials such as CuO, SiC, a-Si, and a metallic substrate has been recently reported to generate reflective colors[14–17]. It is worth pointing out that the thickness of the lossy dielectric layer is generally tens of nanometers, which is much thinner than the dielectric layer with hundreds of nanometers in the conventional MDM structure. In addition, the high refractive index and thin thickness of the introduced lossy dielectric layer endow this simple structure capable of highly improved angular tolerance while simplifying the manufacturing process and enabling an ultracompact device. Different from the typical F-P resonance supported by the MDM structure, the color generation mechanism of this structure originates from the strong resonance excited by the large optical absorption coefficient of the lossy dielectric layer and the concomitant nontrivial phase transition generated by the reflection at the boundary between the lossy dielectric layer and the metallic layer[18,19]. However, the realized ultrathin thickness and excellent angle-insensitive property of the currently reported lossy dielectric-metal structures work on the premise of sacrificing color saturation in conjunction with gamut, which inevitably hinders their practical application.

Here, a thorough theoretical analysis of the color generation mechanism for a lossy dielectric-metal structure [hydrogenated amorphous silicon (a-Si:H)-aluminum (Al) structure as an example] is carried out to comprehend the factors that affect the saturation of output colors. Through the analysis, high color saturation can be realized by choosing a lossy dielectric material with an appropriate complex refractive index. However, it is quite difficult to find a dielectric material with a satisfactory complex refractive index in nature, since material properties are inherently unchangeable. Herein, we propose a new scheme by exploiting a hybrid lossy dielectric layer that comprises two thin layers of a-Si:H and magnesium hydride (MgH_2) with different complex refractive indices. According to the effective medium theory (EMT), the ultrathin MgH_2-a-Si:H hybrid lossy dielectric layer is equivalent to a quasi-homogeneous layer with a tunable effective complex refractive index by simply adjusting the thicknesses of two layers. Through rigorous numerical simulations, it is demonstrated that the proposed color filter has the capability of highly enhanced color saturation and a wide color gamut. Meanwhile, the proposed color filter can retain invariable output color at the incident angle within the range of ±60°. Furthermore, MgH_2 is known to feature an unstable chemical property, leading to an interconversion with Mg in the presence of hydrogen and oxygen. By taking advantage of this characteristic of MgH_2, the proposed color filter can generate dynamically tunable output colors.

2. Results and Discussion

2.1. Theoretical analysis of the color filter based on the lossy dielectric-metal structure

To explore the color generation mechanism of the color filter based on a lossy dielectric-metal structure and the corresponding key factors affecting the output color, a theoretical model is constructed by focusing on the influence of the complex refractive index of the lossy dielectric layer on the reflectance spectrum of the color filter. As illustrated in Fig. 1(a), the constructed color filter is composed of a lossy dielectric layer and an Al substrate. The complex refractive indices of air, the lossy dielectric layer, and the Al substrate are denoted as $N_1=1$, $N_2=n_2+ik_2$, and $N_3=n_3+ik_3$, respectively. The thickness of the lossy dielectric layer is denoted as h. When the light is incident on the lossy dielectric layer from the air at an angle θ_1, the reflection coefficient of this structure can be expressed by the Fresnel-Airy formula as[19,20]

$$r=\frac{r_{12}+r_{23}e^{2i\beta}}{1+r_{12}r_{23}e^{2i\beta}}, \tag{1}$$

where $\beta=2\pi=\lambda N_2 h\cos\theta_2$, θ_2 is the refraction angle, r_{ij} is the polarization-dependent Fresnel coefficient, i and j are integers that vary from 1 to 3 corresponding to the layer 1 to 3 belonging to the color filter structure. The Fresnel coefficients for the s- and p-polarized incident light are given by

$$r_{ij}^{s}=\frac{N_i\cos(\theta_i)-N_j\cos(\theta_j)}{N_i\cos(\theta_i)+N_j\cos(\theta_j)}, \tag{2}$$

$$r_{ij}^{p}=\frac{N_j\cos(\theta_i)-N_i\cos(\theta_j)}{N_j\cos(\theta_i)+N_i\cos(\theta_j)}. \tag{3}$$

By Snell's law, the angle θ_2 is given by $\theta_2=\arcsin[n_1\sin(\theta_1)/n_2]$. The reflectivity of the color filter can be expressed as $R=|r|^2$[20].

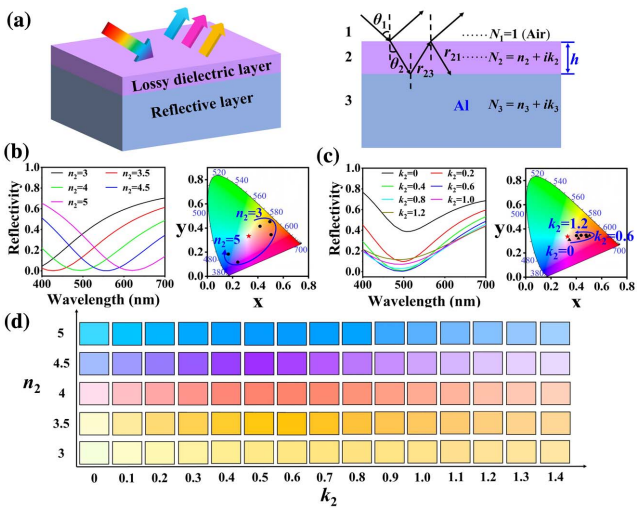

Fig. 1. (a) Schematic diagram of the color filter based on a lossy dielectric-metal structure; (b) reflectance spectra and chromaticity coordinates with increasing n_2 for a fixed k_2 of 0.6; (c) reflectance spectra and chromaticity coordinates with increasing k_2 for a fixed n_2 of 4; (d) color palettes with varying n_2 and k_2.

According to the above equations, the reflectivity of the lossy dielectric-metal structure is closely related to the complex refractive index of the lossy dielectric layer. To understand the effect of its complex refractive index on the total reflectivity, we calculate the reflectivity when the real part n_2 and the imaginary part k_2 of the complex refractive index vary. The thickness h of the lossy dielectric layer is set as 20 nm, and the incident angle θ_1 is maintained at 0°. Figure 1(b) shows the reflectance spectra and the corresponding chromaticity coordinates in the standard International Commission on Illumination (CIE) 1931 chromaticity diagram when n_2 increases from 3 to 5 for a fixed k_2 of 0.6. It can be observed that as n_2 increases, the resonance wavelength gradually redshifts, which can be understood from the satisfied phase condition. According to Eq. (1) and $\beta = (2\pi/\lambda)N_2 h \cos\theta_2$, the resonance condition occurs when $\beta = 2m\pi$, where m is an integer. With all other variables remaining unchanged, the increased n_2 must be accompanied with a redshifted λ to satisfy the resonance condition. As a result, the corresponding color gradually changes from yellow to magenta, and finally to cyan, suggesting that n_2 mainly determines the color hue. Figure 1(c) depicts the variation of the reflectance spectra with augmenting k_2 when $n_2 = 4$. As k_2 varies from 0 to 1.2, the location of the resonance wavelength hardly changes, while the suppression ratio at the resonance wavelength changes severely, thus leading to a drastic variation in color saturation. This clearly exhibits that the chromaticity coordinate gradually moves away from the white point (denoted by a red star) with increasing k_2 from 0 to 0.6, corresponding to gradually enhanced color saturation. However, as k_2 continuously increases from 0.6 to 1.2, the chromaticity coordinate gradually approaches the white point, indicating the deterioration of the color saturation. In order to directly see the impact of the complex refractive index on the colors, additional simulations are performed to examine the reflectance spectra under various combinations of k_2 and n_2, and the corresponding colors are shown in a 2D grid, with x being k_2, and y being n_2, as shown in Fig. 1(d). As n_2 increases from 3 to 5, the color changes from yellow to cyan, indicating that n_2 mainly determines the color hue. It can also be observed that k_2 mainly determines the color saturation, and highly saturated full colors can be achieved within the range of $k = 0.3$–0.8. In light of the above thorough theoretical analysis, it can hence be concluded that the material of the lossy dielectric layer should be selected to feature the complex refractive index with various n_2 to realize different color hues and an imaginary part k_2 of about 0.3–0.8 to get high color saturation.

2.2. Proposed ultrathin color filter with enhanced color saturation exploiting EMT

As a-Si:H features an ultrahigh real part of the complex refractive index in the visible region, we consider using it as the lossy dielectric layer. Figure 2(a) shows the complex refractive index of a-Si:H and the simulated reflectance spectra of the a-Si:H-Al structure using a finite-difference time-domain (FDTD) method-based tool. The thickness of the a-Si:H layer is determined to be 10, 19, and 26 nm to create the subtractive primary

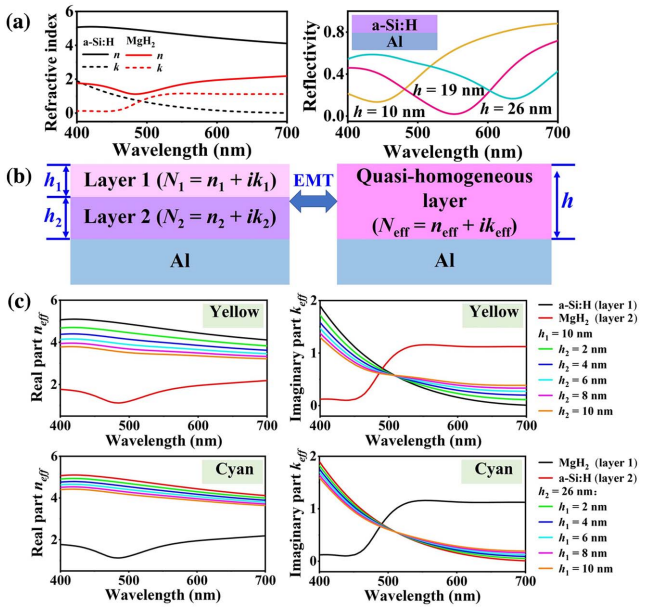

Fig. 2. (a) Complex refractive index of a-Si:H and MgH_2 and reflectance spectra of CMY filters based on the a-Si:H-Al structure; (b) equivalent conversion relationship between hybrid lossy and quasi-homogeneous dielectric layer based on EMT; (c) calculated effective complex refractive indices of the MgH_2-a-Si:H layer with different thicknesses of MgH_2.

colors of cyan, magenta, and yellow (CMY), respectively. Except for the magenta filter, both the yellow and cyan filters have relatively high reflectivity at the resonance wavelengths. Such a low suppression ratio in the reflectance spectra inevitably forms low color saturation. The reason is that the imaginary part of the complex refractive index of a-Si:H is much larger than the desired $k = 0.3$–0.8 with wavelengths shorter than 500 nm, while it is much smaller than that with wavelengths longer than 600 nm. Note that the observed low suppression ratios of the yellow and cyan filters originating from unsatisfactory k are entirely consistent with our previous theoretical predictions.

To enhance the color saturation of the cyan and yellow filters, the imaginary part of the lossy dielectric layer is required to be elaborately adjusted in the targeted wavelength range. Here, we take advantage of EMT to effectively tune the complex refractive index of the lossy dielectric layer, in which EMT refers to a theoretical model indicating that two stacked dielectric layers with ultrathin thicknesses can be equivalent to a quasi-homogeneous dielectric layer with an effective complex refractive index. As illustrated in Fig. 2(b), a dual-layer structure comprising a dielectric layer 1 (thickness of h_1 and complex refractive index of $N_1 = n_1 + ik_1$) and a dielectric layer 2 (thickness of h_2 and complex refractive index of $N_2 = n_2 + ik_2$) can be regarded as a quasi-homogeneous dielectric layer with a thickness of h ($h = h_1 + h_2$) and an effective complex refractive index denoted as $N_{\text{eff}} = n_{\text{eff}} + ik_{\text{eff}}$, as long as the thicknesses of the two dielectric layers are sufficiently small compared to the wavelength of interest. The effective complex refractive index N_{eff} can be approximately calculated according to the simplified analytical expression by EMT[21,22],

$$N_{\text{eff}}=\sqrt{\frac{h_1}{h_1+h_2}N_1^2+\frac{h_2}{h_1+h_2}N_2^2}. \tag{4}$$

According to Eq. (4), it is easy to find that the effective complex refractive index N_{eff} is an intermediate value between the complex refractive indices of the two lossy dielectric layers.

According to our theoretical studies, the lossy dielectric layer should have a large n and k in the ideal range of 0.3–0.8 so that highly saturated full colors can be obtained. As shown in Fig. 2(a), MgH_2, which has the large n and k with a trend opposite that of a-Si:H, is meticulously chosen to combine with a-Si:H to form a quasi-homogeneous dielectric layer close to the ideal value of k. Theoretically, the relative position of the two lossy dielectric layers shall not affect the effective complex refractive index based on the EMT, and it is found in real practice that changing the stacking sequence of the two lossy dielectric layers does not have a large effect on the color hue, yet the color saturation is affected to some extent, as shown in Fig. 3(a). To ensure that the obtained color filters have high color saturations, the stacking sequence of the two layers of a-Si:H and MgH_2 in the proposed color filters is elaborately adjusted. For the yellow filter, the a-Si:H layer is chosen as layer 1, while for the cyan filter, the MgH_2 layer is chosen as layer 1. Furthermore, the thicknesses of a-Si:H layers for the yellow and cyan filters are fixed to 10 and 26 nm, respectively, to maintain the resonance wavelengths relatively stable to render changeless output colors. To obtain the desired k, Fig. 2(c) plots the calculated effective complex refractive indices of MgH_2-a-Si:H lossy dielectric layers by varying the thickness of MgH_2 layer from 2 to 10 nm. Through the rigorous numerical simulations, it is confirmed that when the thickness of the MgH_2 layer is set to 4 nm, appropriate effective complex refractive indices can be obtained for both yellow and cyan filters.

Figure 3(a) shows the simulated reflectance spectra and corresponding CIE 1931 chromaticity coordinates of the yellow and cyan filters with 4-nm thick MgH_2 layers involved for two different stacking cases, as compared with the cases without MgH_2 layers. The suppression ratios at resonance wavelengths of both the proposed yellow (the a-Si:H layer as layer 1) and cyan (the MgH_2 layer as layer 1) filters based on MgH_2-a-Si:H lossy dielectric layers are observed to be plainly enhanced compared to the other cases. Naturally, the proposed color filters enable significant improvement in color saturation. We further calculate the color gamut of the color filters based on a single a-Si:H layer and the proposed structure, as displayed in Fig. 3(b). The proposed structure empowers a wider color gamut, which is 38.9% wider than that of the structure based on a single a-Si:H layer. Note that the thickness of the MgH_2 layer is extremely thin, indicating that the proposed color filter can significantly improve the color saturation and enlarge the color gamut while still maintaining the advantage of ultrathin performance. Considering that the lossy dielectric layer-based thin-film color filter usually features good angular tolerance, we evaluate the angular properties of our proposed color filter.

Figure 4(a) illustrates the angular responses of the proposed CMY filters for s-, p-polarized, and unpolarized incident light, respectively. Here, the hybrid lossy dielectric layer of the magenta filter is composed of a 6-nm thick MgH_2 layer as layer 1 and a 19-nm thick a-Si:H layer as layer 2. For s-polarized light, the reflectance spectra of the CMY filters remain almost invariant in terms of resonance wavelength, reflectivity, suppression ratio, and bandwidth with the incident angle θ_1 increasing

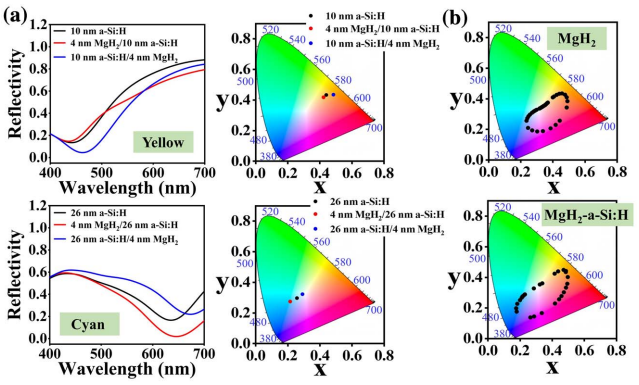

Fig. 3. (a) Reflectance spectra and chromaticity coordinates of yellow and cyan filters without and with the MgH_2 layer in different stacking cases; (b) color gamut of the structure based on a single a-Si:H layer and the proposed structure.

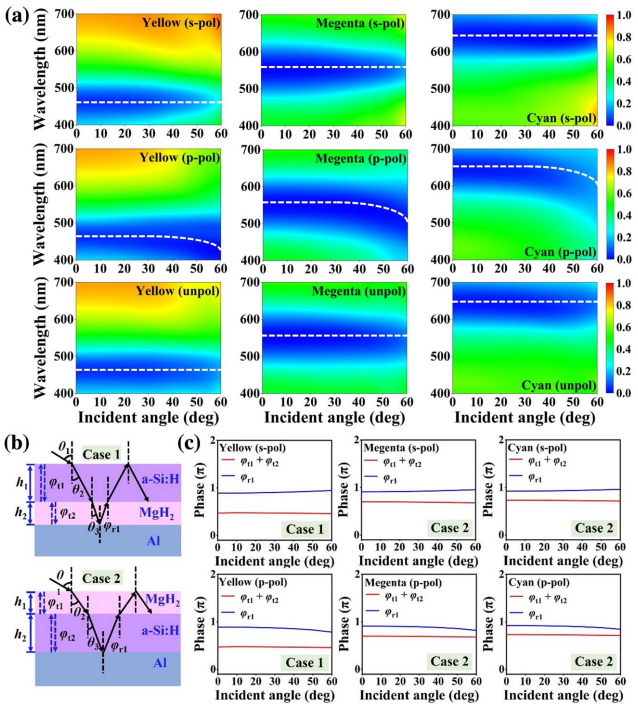

Fig. 4. (a) Reflectance spectra of CMY filters under s-, p-polarized, and unpolarized light illumination when the incident angle increases; (b) schematic diagram of the phases involved in two cases based on different combination orders of MgH_2 and a-Si:H lossy dielectric layers; (c) propagation and reflection phases of the CMY filters as a function of the incident angle under s- and p-polarized light illumination.

from 0° to 60°, implying angle-insensitive color outputs. For p-polarized light, the resonance wavelength undergoes a slight blueshift when the incident angle exceeds 50°. Nonetheless, for unpolarized light, the CMY filters provide unchanging color within the incident angle of 60°, demonstrating the advantage of the proposed color filter for the angle-invariant color response.

Furthermore, the underlying mechanism in regard to the obtained large angular tolerance of the proposed color filter is scrutinized by calculating the phase changes under different incident angles. We inspect two structures, as shown in Fig. 4(b), including Case 1 for a-Si:H as layer 1 and MgH_2 as layer 2 (yellow filter) and Case 2 for MgH_2 as layer 1 and a-Si:H as layer 2 (magenta and cyan filters). Here, φ_{t1} and φ_{t2} are the round-trip propagation phases in two lossy dielectric layers, respectively. It is worth noting that the thickness of the MgH_2 layer is extremely small, so the propagation phase shift related to the incident angle dominantly stems from the a-Si:H layer. φ_{r1} represents the reflection phase that occurs at the interface between the lossy dielectric layer and the Al substrate. The reflection phase between the dielectric layers is extremely small and thus is ignored here. Figure 4(c) plots the dependence of the propagation phases ($\varphi_{t1} + \varphi_{t2}$) and reflection phase ($\varphi_{r1}$) under s- and p-polarized light illumination on the incident angle (θ_1) for the CMY filters at their resonance wavelengths of 650, 560, and 463 nm. The propagation phase shift is approximately invariant when increasing the incident angle for both s- and p-polarized light, which occurs because even though the incident angle alters a lot, the refraction angle minimally varies due to the high real part of the complex refractive index of a-Si:H. For the reflection phase, it remains almost unchanged for s-polarized light but changes slightly for p-polarized light at the angle of incidence exceeding 50°. The phase analysis well accounts for the reason underlying the observed angle-invariant properties of the proposed color filter.

2.3. Dynamic color tuning property

The proposed color filter has the potential to render dynamic color tuning property, as the contained MgH_2 is a chemically unstable material that can be transformed from a dielectric state to the metallic state of Mg via a simple dehydrogenation reaction[23,24]. The detailed mutual conversion process is described as follows: MgH_2 desorbs hydrogen atoms under catalysts and the hydrogen atoms combine with oxygen to form water, finally converting into Mg. Similarly, Mg undergoes the hydrogen absorption reaction in the presence of hydrogen, thereby reconverting to MgH_2. Taking advantage of this active chemical property, the hybrid layer in the proposed color filter can experience the interconversion between MgH_2-a-Si:H and Mg-a-Si:H layer under dehydrogenation/hydrogen absorption, as shown in Fig. 5(a).

To further verify the dynamic color tuning property, the reflectance spectra and corresponding CIE 1931 chromaticity coordinates before and after conversion of the top MgH_2 layer of the cyan and magenta filters have been investigated. As presented in Figs. 5(b) and 5(c), for the cyan and magenta filters, the

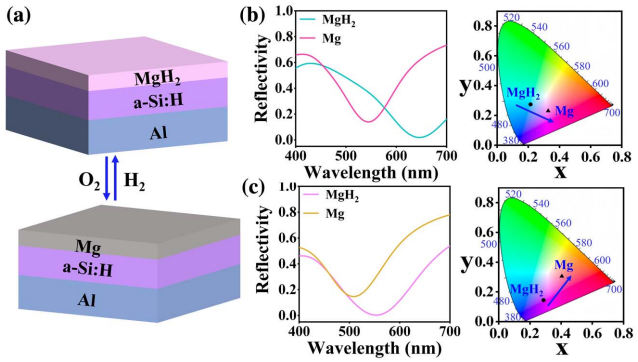

Fig. 5. (a) Schematic diagram of the proposed color filter with regard to the dynamic interconversion in the top layer between MgH_2 and Mg; reflectance spectra and corresponding chromaticity coordinates of (b) the cyan filter and (c) the magenta filter when the top layer of MgH_2 is converted to Mg.

resonance wavelengths significantly blueshift when MgH_2 is converted to Mg, resulting in the output colors changing from cyan to magenta and magenta to yellow, respectively. The observed color tuning property is ascribed to the joint effect of the reduction of the dielectric layer thickness and the change of the resonance mode. Concerning the resonance mode, as the top layer of MgH_2 is converted into Mg, the proposed color filter turns into an MDM structure, which enables a strong suppression in reflection via a typical F-P resonance. Hence, the proposed color filter is confirmed to allow for dynamic tuning of output color, which promotes it to be applied in frontier fields such as dynamic display and high-density information storage.

3. Conclusion

In conclusion, a high-performance ultrathin color filter is proposed by exploiting an EMT-based MgH_2-a-Si:H hybrid lossy dielectric layer. Through theoretical analysis, the real part of the complex refractive index of the lossy dielectric layer is confirmed to determine the resonance wavelength in correspondence to color hue, whereas the imaginary part dominantly affects the reflection suppression ratio related to the color saturation. To enhance the color saturation, we adopt the MgH_2-a-Si:H lossy dielectric layer to freely tune the imaginary part according to EMT. It is verified that the proposed ultrathin color filter is capable of providing significantly enhanced color saturation by merely adding a few-nanometer thick MgH_2 layer. Compared with the typical color filter based on the a-Si:H-Al structure, the color gamut of the proposed color filter can be greatly enlarged by 38.9% and can provide stable and invariable high-saturation output color within the incident angle range of ±60°, corresponding to a large angular tolerance. Finally, by utilizing the mutual conversion of MgH_2 and Mg, the proposed color filter possesses the dynamic color tuning property. The proposed scheme is expected to provide an effective solution for realizing an ultracompact optical display device with high color saturation, wide color gamut, large angular tolerance, and dynamic color tunability.

Acknowledgement

This work was supported by the Natural Science Foundation of Shandong Province (No. ZR2019BF013) and the National Natural Science Foundation of China (Nos. 62005095 and 61905091).

References

1. B. Yang, H. Cheng, S. Chen, and J. Tian, "Structural colors in metasurfaces: principle, design and applications," Mater. Chem. Front. **3**, 750 (2019).
2. T. Lee, J. Jang, H. Jeong, and J. Rho, "Plasmonic-and dielectric-based structural coloring: from fundamentals to practical applications," Nano Converg. **5**, 1 (2018).
3. P. Vukusic, J. R. Sambles, C. R. Lawrence, and R. J. Wootton, "Structural colour-now you see it now you don't," Nature **410**, 36 (2001).
4. M. Seo, J. Kim, H. Oh, M. Kim, I. U. Baek, K. D. Choi, J. Y. Byun, and M. Lee, "Printing of highly vivid structural colors on metal substrates with a metal-dielectric double layer," Adv. Opt. Mater. **7**, 1900196 (2019).
5. D. Inoue, A. Miura, T. Nomura, H. Fujikawa, K. Sato, N. Ikeda, D. Tsuya, Y. Sugimoto, and Y. Koide, "Polarization independent visible color filter comprising an aluminum film with surface-plasmon enhanced transmission through a subwavelength array of holes," Appl. Phys. Lett. **98**, 093113 (2011).
6. Z. Dong, J. Ho, Y. F. Yu, Y. H. Fu, R. Paniagua-Dominguez, S. Wang, A. I. Kuznetsov, and J. K. W. Yang, "Printing beyond sRGB color gamut by mimicking silicon nanostructures in free-space," Nano Lett. **17**, 7620 (2017).
7. W. Yue, S. Gao, S. S. Lee, E. S. Kim, and D. Y. Choi, "Highly reflective subtractive color filters capitalizing on a silicon metasurface integrated with nanostructured aluminum mirrors," Laser Photonics Rev. **11**, 1600285 (2017).
8. K. Aydin, V. E. Ferry, R. M. Briggs, and H. A. Atwater, "Broadband polarization-independent resonant light absorption using ultrathin plasmonic super absorbers," Nat. Commun. **2**, 517 (2011).
9. J. Zhao, M. Qiu, X. Yu, X. Yang, W. Jin, D. Lei, and Y. Yu, "Defining deep-subwavelength-resolution, wide-color-gamut, and large-viewing-angle flexible subtractive colors with an ultrathin asymmetric Fabry-Perot lossy cavity," Adv. Opt. Mater. **7**, 1900646 (2019).
10. K. Feng, Q. Li, J. Liu, Y. Wang, N. Chen, Y. Li, and Y. Bu, "All-dielectric thin films based on single silicon materials for angle-insensitive structural colors," Opt. Lett. **46**, 5161 (2021).
11. Z. Li, S. Butun, and K. Aydin, "Large-area, lithography-free super absorbers and color filters at visible frequencies using ultrathin metallic films," ACS Photonics **2**, 183 (2015).
12. Z. Yang, Y. Zhou, Y. Chen, Y. Wang, P. Dai, Z. Zhang, and H. Duan, "Reflective color filters and monolithic color printing based on asymmetric Fabry-Perot cavities using nickel as a broadband absorber," Adv. Opt. Mater. **4**, 1196 (2016).
13. C. Liu, G. Wang, L. Zhang, F. Fan, X. Zhang, Y. Fu, and T. Wang, "Dynamic color display with viewing-angle tolerance based on the responsive asymmetric Fabry-Perot cavity," ACS Appl. Mater. Interfaces **14**, 7200 (2022).
14. H. Pan, Z. Wen, Z. Tang, G. Xu, X. Pan, Q. Xu, Y. Lu, H. Xu, Y. Sun, N. Dai, and J. Hao, "Wide gamut angle-insensitive structural colors based on deep-subwavelength bilayer media," Nanophotonics **9**, 3385 (2020).
15. Z. Lin, S. Zhang, M. Zheng, Y. Long, Z. Yang, Y. Zhou, and H. Duan, "Silicon carbide film-based Fabry-Pérot cavity resonance-enhanced absorption and its application for color filters," Opt. Mater. **96**, 109370 (2019).
16. S. Ayas, G. Bakan, E. Ozgur, K. Celebi, G. Torunoglu, and A. Dana, "Colorimetric detection of ultrathin dielectrics on strong interference coatings," Opt. Lett. **43**, 1379 (2018).
17. Z. Wen, J. Lu, W. Yu, H. Wu, H. Xie, X. Pan, Q. Xu, Z. Zhou, C. Tan, D. Zhou, C. Liu, Y. Sun, N. Dai, and J. Hao, "Dynamically reconfigurable subwavelength optical device for hydrogen sulfide gas sensing," Photonics Res. **9**, 2060 (2021).
18. K. T. Lee, S. Seo, J. Y. Lee, and L. J. Guo, "Strong resonance effect in a lossy medium-based optical cavity for angle robust spectrum filters," Adv. Mater. **26**, 6324 (2014).
19. M. A. Kats, R. Blanchard, P. Genevet, and F. Capasso, "Nanometre optical coatings based on strong interference effects in highly absorbing media," Nat. Mater. **12**, 20 (2013).
20. M. A. Kats and F. Capasso, "Optical absorbers based on strong interference in ultra-thin films," Laser Photonics Rev. **10**, 735 (2016).
21. Z. Yang, C. Ji, D. Liu, and L. J. Guo, "Enhancing the purity of reflective structural colors with ultrathin bilayer media as effective ideal absorbers," Adv. Opt. Mater. **7**, 1900739 (2019).
22. C. Della Giovampaola and N. Engheta, "Digital metamaterials," Nat. Mater. **13**, 1115 (2014).
23. Y. Chen, X. Duan, M. Matuschek, Y. Zhou, F. Neubrech, H. Duan, and N. Liu, "Dynamic color displays using stepwise cavity resonators," Nano Lett. **17**, 5555 (2017).
24. X. Duan, S. Kamin, and N. Liu, "Dynamic plasmonic colour display," Nat. Commun. **8**, 14606 (2017).